JACS
JOURNAL OF THE AMERICAN CHEMICAL SOCIETY
Communication
pubs.acs.org/JACS

Consequences of Inducing Intrinsic Disorder in a High-Affinity Protein–Protein Interaction

Grigorios Papadakos,[†] Amit Sharma,[‡] Lorna E. Lancaster,[§] Rebecca Bowen,[∥,#] Renata Kaminska,[†] Andrew P. Leech,[∥] Daniel Walker,[⊥] Christina Redfield,[†] and Colin Kleanthous*[,†]

[†]Department of Biochemistry, University of Oxford, South Parks Road, Oxford OX1 3QU, United Kingdom
[‡]Astbury Centre for Structural Molecular Biology, University of Leeds, Leeds LS2 9JT, United Kingdom
[§]School of Life Sciences, University of Lincoln, Brayford Pool, Lincoln LN6 7TS, United Kingdom
[∥]Department of Biology, University of York, Heslington Road, York YO10 5DD, United Kingdom
[⊥]Institute of Infection, Immunity and Inflammation, College of Medical, Veterinary and Life Sciences, University of Glasgow, Glasgow G12 8AT, United Kingdom

Supporting Information

ABSTRACT: The kinetic and thermodynamic consequences of intrinsic disorder in protein–protein recognition are controversial. We address this by inducing one partner of the high-affinity colicin E3 rRNase domain–Im3 complex ($K_d \approx 10^{-12}$ M) to become an intrinsically disordered protein (IDP). Through a variety of biophysical measurements, we show that a single alanine mutation at Tyr507 within the hydrophobic core of the isolated colicin E3 rRNase domain causes the enzyme to become an IDP (E3 rRNase^{IDP}). E3 rRNase^{IDP} binds stoichiometrically to Im3 and forms a structure that is essentially identical to the wild-type complex. However, binding of E3 rRNase^{IDP} to Im3 is 4 orders of magnitude weaker than that of the folded rRNase, with thermodynamic parameters reflecting the disorder-to-order transition on forming the complex. Critically, pre-steady-state kinetic analysis of the E3 rRNase^{IDP}–Im3 complex demonstrates that the decrease in affinity is mostly accounted for by a drop in the electrostatically steered association rate. Our study shows that, notwithstanding the advantages intrinsic disorder brings to biological systems, this can come at severe kinetic and thermodynamic cost.

Intrinsically disordered proteins (IPDs) are found in all domains of life, where they play central roles in a multitude of biological processes, including transcription, translation, cell division, and cell death.[1] IDPs are also implicated in a number of human diseases, such as cancer, Alzheimer's disease, Parkinson's disease, and type II diabetes.[2] The functional repertoire of IDPs is similarly diverse, ranging from flexible linkers between domains, sites of post-translational modification, chaperones for proteins and nucleic acids, hubs in protein–protein interaction (PPI) networks, and membrane translocation modules.[3] IDP assembly is critical to the recently described phenomenon of liquid-to-liquid phase transitions within cells and has been exploited in the generation of novel biomaterials.[4] Given the importance of IDPs to biology, medicine, and biotechnology, there is great interest in understanding their mechanisms of association with other macromolecules. Since IDPs have been retained in biological systems over evolutionary time, this implies that they endow these systems with particular advantages over their globular counterparts.[3b] One of the often cited advantages of IDPs in PPIs is their faster association rate, due to a larger capture radius, the so-called "fly-casting" mechanism, and fewer encounters on the path to the final complex.[5] However, beyond surveys of association rate data for IDP and globular protein complexes and theoretical predictions, there has been no direct experimental test of this effect, presumably because of the difficulty in comparing the *same* PPI for a globular and IDP complex. The present work set out to address this problem by using the colicin ribonuclease E3 and its specific immunity protein, Im3.

Colicin E3 (ColE3) is a ribosomal RNase (rRNase) toxin released by *Escherichia coli* cells to kill their neighbors during times of environmental stress. The 12-kDa E3 rRNase domain is delivered to the cytoplasm of susceptible bacteria, where it cleaves the phosphodiester bond between A1493 and G1494 within the decoding center of the ribosomal A-site, leading to the inhibition of protein synthesis and cell death.[6] ColE3-producing bacteria are protected against the action of the rRNase and hence suicide by the 9.8-kDa immunity protein Im3. Im3 binds with very high affinity ($K_d = 10^{-12}$ M, pH 7.0, 200 mM NaCl, and 25 °C) to the isolated E3 rRNase domain, only dissociating from the enzyme during colicin import.[7,8] Interestingly, the Im3–E3 rRNase complex has some features associated with IDP complexes: Im3 makes contact with long, contiguous segments of the E3 rRNase polypeptide, including the N-terminal α-helix, a long linker sequence that lacks regular secondary structure, and two short strands of β-sheet.[9]

Previously, we have shown, using far-UV circular dichroism (CD) and tryptophan emission fluorescence spectroscopy, that an alanine mutant of Tyr507 within the hydrophobic core of the rRNase destabilizes the enzyme.[10] Here, closer analysis of this mutant by differential scanning calorimetry (DSC), near-UV CD, analytical ultracentrifugation (AUC), and high-field NMR spectroscopy indicated that Y507A E3 rRNase was unfolded at room temperature and hence had become a *de facto* IDP (E3

Received: December 11, 2014
Published: April 9, 2015

DOI: 10.1021/ja512607r
J. Am. Chem. Soc. 2015, 137, 5252–5255

rRNase^{IDP}; Figure S1). In fact, a significant proportion of the ColE3 rRNase domain is predicted to be disordered (35 and 50% using PONDR-VLXT and PRDos, respectively), a consequence of its high glycine, lysine, and proline contents (17, 18, and 9%, respectively). It is perhaps unsurprising, therefore, that although the E3 rRNase is clearly a folded domain ($\Delta G_{stabilization}$ = −9.2 kcal/mol by DSC; Figure S1), a single Tyr-to-Ala mutation within its hydrophobic core is sufficient to render it an IDP. We determined the hydrodynamic radius of E3 rRNase^{IDP} by NMR spectroscopy (25.6 Å) and found it midway between those of the native domain (20.1 Å) and E3 rRNase unfolded in 8 M urea (30.2 Å), suggesting that, like other IDPs,[11] E3 rRNase^{IDP} is more compact than the urea-denatured state. Its compact shape might arise from its high glycine and proline contents, as previously observed for IDPs.[12a,b] No changes in the hydrodynamic radius of the E3 rRNase^{IDP} were observed across a range of 0−500 mM NaCl, so, unlike other IDPs,[12a,c] its relative compactness is probably not due to favorable intramolecular charge−charge interactions.

We next examined the ability of E3 rRNase^{IDP} to bind Im3. Tryptophan fluorescence emission spectroscopy, sedimentation velocity AUC, and $^{1}H-^{15}N$ HSQC NMR spectroscopy showed that E3 rRNase^{IDP} bound Im3 stoichiometrically (Figure S2A−C). We also crystallized the E3 rRNase^{IDP}−Im3 complex and solved its structure at 2.97 Å resolution by molecular replacement (see Table S1 for refinement statistics). The root-mean-square deviation for backbone atoms of a structural superposition of the wild-type (WT) and E3 rRNase^{IDP} was 0.36 Å (for 96 residues), indicating that, upon binding Im3, the E3rRNase^{IDP} folds to a conformation identical to that of the WT protein (Figure 1A). Indeed, every hydrogen-bonding, hydrophobic, and electrostatic interaction associated with the binding interface of the complex is preserved. The major differences between the structures are localized to the mutation site within the hydrophobic core of the E3 rRNase, although even here the backbone conformations of WT E3 rRNase and the E3 rRNase^{IDP} are nearly identical, emphasized by the conserved hydrogen-bonding interactions involving the main-chain atoms of residue 507 with Trp498 (Figure 1A). The only substantial differences between the WT and mutant complexes are the creation of a 213 Å^3 cavity (Figure 1B), accounting for 3.4% of the hydrophobic core of the E3 rRNase, and the loss of two ordered water molecules that are coordinated to the phenolic hydroxyl of Tyr507 (Figure 1A). We conclude that it is the loss of these interactions which renders the unliganded E3 rRNase^{IDP} predominantly unfolded at room temperature. We note that complexes involving IDPs are sometimes "frustrated",[13] and so a cavity within the core of the E3 rRNase^{IDP} merely represents another form of frustration.

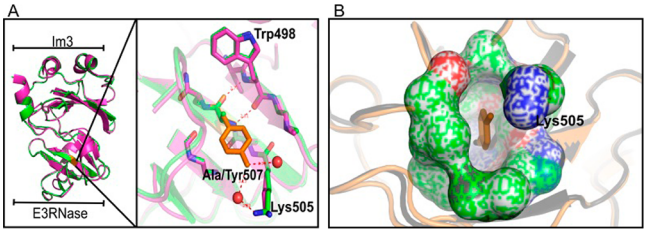

Figure 1. E3 rRNase^{IDP} (Y507A) folds into a native-like structure upon binding to its cognate partner Im3. (A) Superposed cartoon models of the wild-type (magenta) and Im3−E3 rRNase^{IDP} complex (green), highlighting the structural similarity between the two complexes (inset), and the ball-and-stick model showing the disposition of residues in a 5 Å sphere around Tyr/Ala507. Also shown are the H-bond interactions of Ala/Tyr507 and associated water molecules that are lost in the alanine mutant. (B) Surface representation of residues in a 5 Å sphere, highlighting the hole created when Tyr507 is substituted for alanine.

Having established that the complex formed between E3 rRNase^{IDP} and Im3 is essentially identical to that formed by the WT enzyme, we embarked on a thermodynamic and kinetic dissection of the complex. Isothermal titration calorimetry (ITC) demonstrated that the thermodynamic consequence of inducing the E3 rRNase to become an IDP (at pH 7.0 and 25 °C) was a 4 orders of magnitude increase in the equilibrium dissociation constant with respect to that of the WT complex: K_d = 28 nM compared to 1.2 pM at 25 °C, pH 7.0, 200 mM NaCl (Figure S2D and Table 1). Concomitant with this decrease in affinity is a complete change in the thermodynamic profile of the complex. Whereas a favorable enthalpy and entropy drive complex formation of the folded proteins, the E3 rRNase^{IDP}−Im3 complex has a strongly disfavored entropy that is compensated by a large increase in the enthalpic component. These thermodynamic features of the E3 rRNase^{IDP}−Im3 complex are typical of binding-induced folding described for many complexes involving IDPs. The large entropic penalty is due to the loss of intramolecular conformational degrees of freedom due to folding, which in this case is only partly compensated by the favorable desolvation of the exposed hydrophobic core of the E3 rRNase (−25 kcal/mol for E3 rRNase^{IDP} compared to +3.2 kcal/mol in the case of the WT E3). The large favorable enthalpy reflects both the noncovalent interactions that stabilize the folded state of the enzyme and the extensive network of interactions between the two proteins at their interface (Table 1). A further striking difference between the E3 rRNase^{IDP}−Im3 and WT complexes is the much weaker ionic strength dependence for the complex involving the IDP. The affinity of WT E3 rRNase for Im3 is reduced by almost 3 orders of magnitude over a NaCl concentration range of 20−500 mM,[8] whereas E3 rRNase^{IDP} affinity is only affected 20-fold.

Table 1. E3 rRNase−Im3 Binding Energetics Determined by ITC[a]

	[NaCl]			
	20 mM	200 mM		500 mM
	E3 rRNase^{IDP}	WT[b]	E3 rRNase^{IDP}	E3 rRNase^{IDP}
ΔH	−41.0 ± 1.6	−13.0	−35.0 ± 6.0	−31.0 ± 4.5
$T\Delta S$	−29.6 ± 1.6	3.2	−24.8 ± 6.2	−21.0 ± 4.6
ΔG	−11.4	−16.2	−10.2	−10.0
K_d (M)	4.0×10^{-9}	1.2×10^{-12}	2.8×10^{-8}	7.2×10^{-8}

[a]Energies expressed in kcal/mol, and all binding experiments performed in 50 mM MOPS−NaOH, pH 7.0, at 25 °C and the indicated salt concentrations. [b]WT, wild-type E3 rRNase values taken from ref 8.

We next investigated the impact of inducing E3 rRNase to become an IDP on the kinetics of complex formation with Im3. The WT complex is characterized by a very rapid, salt-dependent bimolecular association ($k_{on} \approx 10^8$ M^{-1} s^{-1}) in 50 mM MOPS-NaOH, 200 mM NaCl, at 25 °C and pH 7.0, and a slow, salt-independent dissociation. In the present work, we measured dissociation of the E3 rRNase^{IDP}−Im3 complex using Alexa^{488}-modified Im3, in which the native cysteine (Cys47) was substituted for serine and a Glu-to-Cys mutation was created at position 53 for Alexa^{488} labeling. Position 53 was chosen, as it is

DOI: 10.1021/ja512607r
J. Am. Chem. Soc. 2015, 137, 5252−5255

distant from the E3 rRNase binding site. ITC experiments indicated that Im3-Alexa^{488} bound E3 rRNase^{IDP} with low nanomolar affinity, as for WT Im3 (data not shown). Competition experiments were set up where the E3 rRNase^{IDP}–Im3-Alexa^{488} complex was incubated with an excess of unlabeled Im3 in 50 mM MOPS–NaOH, pH 7.0, at various NaCl concentrations. The release of Im3-Alexa^{488} was followed either by fluorescence anisotropy in a stopped-flow device (T-mode) upon excitation at 470 nm or by absorbance of released Im3-Alexa^{488} at 492 nm following nickel-affinity chromatography. Biphasic dissociation profiles were obtained by both approaches, in contrast to the single phase observed for the WT complex (Figure 2).[8] The biphasic traces were fitted to a double

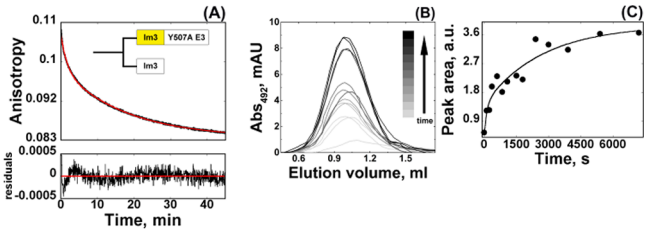

Figure 2. Dissociation of the E3 rRNase^{IDP}–Im3 complex measured through competition with Im3. (A) Time dependence of the anisotropy change for the dissociation of a 0.5 μM E3 rRNase^{IDP}–Im3-Alexa^{488} complex chased by 5 μM unlabeled Im3. Upon excitation at 470 nm, the anisotropy of Im3-Alexa^{488} was monitored in T-mode, with a 515 nm cutoff filter set before each detector. The data were fit to a double exponential equation (red, calculated from eq 1 in the Supporting Information). (B) Time dependence of the Ni-NTA elution peak corresponding to the released Im3-Alexa^{488} (492 nm) upon dissociation of a 2 μM E3 rRNase^{IDP}–Im3-Alexa^{488} complex chased by 20 μM unlabeled Im3. (C) Fit of the integrated areas in (B) to a double exponential equation (eq 1 in the Supporting Information). All experiments were performed in 50 mM MOPS–NaOH, 200 mM NaCl, pH 7.0, at 25 °C.

Table 2. E3 rRNase^{IDP}–Im3 Association and Dissociation Kinetic Rates[a]

[NaCl]:	20 mM	200 mM	500 mM
k_{on} ($\times 10^5$ M^{-1} s^{-1})	40 ± 3.2	4.4 ± 0.2	1.2 ± 0.02
k^1_{off} ($\times 10^{-4}$ s^{-1})	2.3 (±1.7)[a]	3.1 (±0.01)[a]	3.8 (±0.02)[a]
		3.7 (±2.4)[b]	
k^2_{off} ($\times 10^{-3}$ s^{-1})	4.6 (±0.08)[a]	6.3 (±0.04)[a]	7.3 (±0.04)[a]
		4.3 (±2.0)[b]	

[a] k_{off} values determined by [a]fluorescence anisotropy and [b]chromatographic release of Im3-Alexa. Experiments performed in 50 mM MOPS–NaOH, pH 7.0, at 25 °C and the indicated salt concentrations. k_{on} and k_{off} for the WT complex in 200 mM NaCl under identical buffer conditions are 1.1×10^8 M^{-1} s^{-1} and 1.5×10^{-4} s^{-1}, respectively.[8]

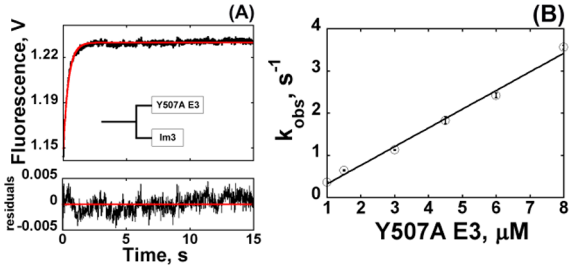

Figure 3. E3 rRNase^{IDP}–Im3 association monitored by stopped-flow fluorescence spectroscopy in 50 mM MOPS–NaOH, 200 mM NaCl, pH 7.0, at 25 °C. (A) Time dependence of the tryptophan fluorescence emission upon excitation at 295 nm under pseudo-first-order conditions: 0.2 μM Im3 mixed with 8 μM E3 rRNase^{IDP}. (B) Dependence of the observed rate constants under pseudo-first-order conditions (tryptophan emission experiments) on the concentration of E3 rRNase^{IDP} and its linear regression (black line, calculated from eq 2 in the Supporting Information), which yields a bimolecular association constant of 4.4×10^5 M^{-1} s^{-1}.

exponential equation from which the amplitudes were estimated to differ by the same magnitude in the two experimental setups (~2.5-fold), suggesting that both experiments were monitoring the same dissociation-induced processes. The average values of the two dissociation rate constants for the E3 rRNase^{IDP}–Im3-Alexa^{488} complex (k^1_{off} and k^2_{off}), corresponding to the higher and lower amplitudes, were 3.4×10^{-4} and 0.5×10^{-4} s^{-1}, respectively, in 50 mM MOPS–NaOH, 200 mM NaCl, at 25 °C and pH 7.0. Both rates were independent of the competing ligand concentration, and both exhibited a mild dependence on NaCl concentration (Table 2). Importantly, both rate constants approximate that of the WT complex under equivalent conditions ($k_{off} = 1.5 \times 10^{-4}$ s^{-1}).[8] We conclude that, while inducing the E3 rRNase to become an IDP increases the complexity of its dissociation mechanism from its complex with Im3, likely involving different conformational states, it has a minimal impact on the overall rate of dissociation.

The association kinetics of E3 rRNase^{IDP} with Im3 was determined using stopped-flow tryptophan fluorescence, capitalizing on the significant enhancement in fluorescence emission that occurs on complex formation (Figure S2A). A single bimolecular step was observed under pseudo-first-order conditions, without any detectable intermediates, from which an apparent association rate constant of 4.4×10^5 M^{-1} s^{-1} was obtained (Figure 3). With regard to the kinetic mechanism of the E3 rRNase^{IDP}–Im3 complex, kinetic modeling using the apparent rate constants for association and dissociation (data not shown) has thus far been unsuccessful in furnishing an equilibrium dissociation constant, from which we infer that additional, spectroscopically silent steps are involved in complex formation. Nevertheless, our results demonstrate that one partner becoming an IDP has a profound impact on the kinetics of complex formation. First and foremost, the association rate constant for the E3 rRNase^{IDP}–Im3 complex decreased by 3 orders of magnitude relative to that of the WT complex under the same conditions (Table 2).[8] This is a particularly striking result, given theoretical predictions suggesting that IDPs have a kinetic advantage in forming protein–protein complexes. However, in this instance, a further contributory factor impacts on association, which is the role of electrostatics. Association of WT E3 rRNase with Im3 is strongly electrostatically driven, demonstrated by the 3 order of magnitude decrease in the association rate constant when the NaCl concentration is increased from 0 to 500 mM.[8] Such strong salt dependence is typical of long-range electrostatic steering, observed in many complexes involving oppositely charged proteins such as barnase–barstar and the colicin E9 DNase–Im9 complexes. The E3 rRNase is a basic protein (pI = 9.9), with an overall charge of +11 [13 Asp + Glu/24 Arg + Lys], while Im3 is acidic, with an overall charge of −14 [20 Asp + Glu/6 Arg + Lys] at neutral pH. Even though the charge state for the E3 rRNase^{IDP} mutant is identical to that for the WT protein, there is now only a modest ionic strength dependence in its

DOI: 10.1021/ja512607r
J. Am. Chem. Soc. 2015, 137, 5252–5255

association rate with Im3, which decreases by only an order of magnitude between 20 and 200 mM NaCl (Table 2).

This implies that the electrostatic steering responsible for enhancing its association with Im3 is reduced on the E3 rRNase^{IDP} mutant becoming an IDP. It has previously been demonstrated that charge complementarity plays a minor role in accelerating the association rates of short IDP fragments binding folded, globular protein partners.[14] In the present case, we see that the same principle applies for a large, highly charged IDP (E3 rRNase^{IDP}) that in its folded state experiences marked electrostatic steering when binding its acidic partner Im3.[8] Yet, taking the complex as an ensemble of rapidly interconverting conformers (Figure S1E), the "polyelectrostatic effect"[15] predicts that rRNase^{IDP} should experience electrostatic steering. Consequently, the formation of a potential encounter Im3−E3 rRNase^{IDP} complex, where the rRNase folds upon binding, cannot be electrostatically driven. For steering to occur, the E3 rRNase needs to be natively folded before associating with Im3. The decrease in k_{on} could reflect the low concentration in the IDP ensemble of a "binding-competent, native-like" conformation of E3 rRNase^{IDP}. In 200 mM NaCl, this species would have to represent 0.4% of the ensemble if it had the same k_{on} as the native E3 rRNase. Such a "native-like" species present in the IDP ensemble would be expected to show the same, very strong electrostatic steering observed for the native protein; this is not observed. Thus, the change in NaCl concentration would have to have opposite effects: increasing salt diminishes electrostatic steering but at the same time increases the population of the binding-competent, native-like state (from 0.03% at 20 mM NaCl to 0.4% at 200 mM NaCl to 0.75% at 500 mM NaCl). These very small populations of a binding-competent state are almost impossible to detect by any biophysical method. Relaxation dispersion methods are often used to detect low-population "excited" states in a conformational ensemble. No evidence for such a species in E3 rRNase^{IDP} could be detected using ^{15}N relaxation dispersion. In addition, no change in the hydrodynamic radius of the IDP ensemble was observed between 0 and 500 mM NaCl.

To date, the kinetic and thermodynamic merits of IDPs in protein−protein complexes have been established via their comparison with folded proteins that bind to the same partner. Our work provides unique insight into the consequences of disorder on a high-affinity complex through direct comparison of the ordered and disordered states binding the same partner. We highlight the possibility that plasticity and larger hydrodynamic radius may actually decrease the association rate by diminishing the influence of charge on the formation of the encounter complex between a highly charged IDP and its folded counterpart. This is in contrast to the "fly-casting" mechanism,[5] which is often used to explain diffusion-limited association rates for IDP complexes.[16]

■ ASSOCIATED CONTENT

Ⓢ Supporting Information

Supplementary Figures S1 and S2, Table S1, and detailed experimental procedures. This material is available free of charge via the Internet at http://pubs.acs.org.

■ AUTHOR INFORMATION

Corresponding Author

*colin.kleanthous@bioch.ox.ac.uk

Present Address

#R.B.: Oxford Nanopore Technologies, Oxford OX4 4GA, U.K.

Notes

The authors declare no competing financial interest.

■ ACKNOWLEDGMENTS

This work was supported by a grant from the Biotechnology and Biological Sciences Research Council of the UK (BB/G020671/1). We acknowledge ESRF ID144 for providing beam time.

■ REFERENCES

(1) (a) Dyson, H. J.; Wright, P. E. *Nat. Rev. Mol. Cell Biol.* **2005**, *6*, 197. (b) Uversky, V. N. *Int. J. Biochem. Cell Biol.* **2011**, *43*, 1090. (c) Uversky, V. N. *Chem. Rev.* **2014**, *114*, 6557. (d) Ward, J. J.; Sodhi, J. S.; McGuffin, L. J.; Buxton, B. F.; Jones, D. T. *J. Mol. Biol.* **2004**, *337*, 635.

(2) (a) Knowles, T. P.; Vendruscolo, M.; Dobson, C. M. *Nat. Rev. Mol. Cell Biol.* **2014**, *15*, 384. (b) Larsen, R. A.; Chen, G. J.; Postle, K. *J. Bacteriol.* **2003**, *185*, 4699. (c) Westermark, P.; Wernstedt, C.; Wilander, E.; Hayden, D. W.; O'Brien, T. D.; Johnson, K. H. *Proc. Natl. Acad. Sci. U.S.A.* **1987**, *84*, 3881. (d) Xue, B.; Uversky, V. N. *J. Mol. Biol.* **2014**, *426*, 1322.

(3) (a) van der Lee, R.; Buljan, M.; Lang, B.; Weatheritt, R. J.; Daughdrill, G. W.; Dunker, A. K.; Fuxreiter, M.; Gough, J.; Gsponer, J.; Jones, D. T.; Kim, P. M.; Kriwacki, R. W.; Oldfield, C. J.; Pappu, R. V.; Tompa, P.; Uversky, V. N.; Wright, P. E.; Babu, M. M. *Chem. Rev.* **2014**, *114*, 6589. (b) Liu, Z.; Huang, Y. *Protein Sci.* **2014**, *23*, 539. (c) Housden, N. G.; Hopper, J. T.; Lukoyanova, N.; Rodriguez-Larrea, D.; Wojdyla, J. A.; Klein, A.; Kaminska, R.; Bayley, H.; Saibil, H. R.; Robinson, C. V.; Kleanthous, C. *Science* **2013**, *340*, 1570.

(4) Toretsky, J. A.; Wright, P. E. *J. Cell Biol.* **2014**, *206*, 579.

(5) Shoemaker, B. A.; Portman, J. J.; Wolynes, P. G. *Proc. Natl. Acad. Sci. U.S.A.* **2000**, *97*, 8868.

(6) (a) Bowman, C. M.; Dahlberg, J. E.; Ikemura, T.; Konisky, J.; Nomura, M. *Proc. Natl. Acad. Sci. U.S.A* **1971**, *68*, 964. (b) Ng, C. L.; Lang, K.; Meenan, N. A.; Sharma, A.; Kelley, A. C.; Kleanthous, C.; Ramakrishnan, V. *Nat. Struct. Mol. Biol.* **2010**, *17*, 1241.

(7) Vankemmelbeke, M.; Zhang, Y.; Moore, G. R.; Kleanthous, C.; Penfold, C. N.; James, R. *J. Biol. Chem.* **2009**, *284*, 18932.

(8) Walker, D.; Moore, G. R.; James, R.; Kleanthous, C. *Biochemistry* **2003**, *42*, 4161.

(9) Carr, S.; Walker, D.; James, R.; Kleanthous, C.; Hemmings, A. M. *Structure* **2000**, *8*, 949.

(10) Walker, D.; Lancaster, L.; James, R.; Kleanthous, C. *Protein Sci.* **2004**, *13*, 1603.

(11) Uversky, V. N. *Biochim. Biophys. Acta* **2013**, *1834*, 932.

(12) (a) Marsh, J. A.; Forman-Kay, J. D. *Biophys. J.* **2010**, *98*, 2383. (b) Tran, H. T.; Mao, A.; Pappu, R. V. *J. Am. Chem. Soc.* **2008**, *130*, 7380. (c) Muller-Spath, S.; Soranno, A.; Hirschfeld, V.; Hofmann, H.; Ruegger, S.; Reymond, L.; Nettels, D.; Schuler, B. *Proc. Natl. Acad. Sci. U.S.A.* **2010**, *107*, 14609.

(13) Jemth, P.; Mu, X.; Engstrom, A.; Dogan, J. *J. Biol. Chem.* **2014**, *289*, 5528.

(14) (a) Shammas, S. L.; Travis, A. J.; Clarke, J. *J. Phys. Chem. B* **2013**, *117*, 13346. (b) Sugase, K.; Dyson, H. J.; Wright, P. E. *Nature* **2007**, *447*, 1021.

(15) (a) Borg, M.; Mittag, T.; Pawson, T.; Tyers, M.; Forman-Kay, J. D.; Chan, H. S. *Proc. Natl. Acad. Sci. U.S.A.* **2007**, *104*, 9650. (b) Mittag, T.; Orlicky, S.; Choy, W. Y.; Tang, X.; Lin, H.; Sicheri, F.; Kay, L. E.; Tyers, M.; Forman-Kay, J. D. *Proc. Natl. Acad. Sci. U.S.A.* **2008**, *105*, 17772.

(16) (a) Chemes, L. B.; Sanchez, I. E.; de Prat-Gay, G. *J. Mol. Biol.* **2011**, *412*, 267. (b) Dogan, J.; Schmidt, T.; Mu, X.; Engstrom, A.; Jemth, P. *J. Biol. Chem.* **2012**, *287*, 34316. (c) Ganguly, D.; Otieno, S.; Waddell, B.; Iconaru, L.; Kriwacki, R. W.; Chen, J. *J. Mol. Biol.* **2012**, *422*, 674. (d) Rogers, J. M.; Steward, A.; Clarke, J. *J. Am. Chem. Soc.* **2013**, *135*, 1415. (e) Shammas, S. L.; Travis, A. J.; Clarke, J. *Proc. Natl. Acad. Sci. U.S.A.* **2014**, *111*, 12055. (f) Arai, M.; Ferreon, J. C.; Wright, P. E. *J. Am. Chem. Soc.* **2012**, *134*, 3792.

DOI: 10.1021/ja512607r
J. Am. Chem. Soc. 2015, 137, 5252−5255